Anchor-based Detection and Height Estimation Framework for Particle Defects on Cathodic Copper Plate Surface

Chen Sun, Qian Wan, Zhaofu Li, Liang Gao,

Xinyu Li and Yiping Gao

School of Mechanical Science and Engineering

Huazhong University of Science and Technology

2022/08

Content

I. Introduction

II. Proposed ADHE Method

III. Experiments

IV. Conclusion

Introduction

■ Defects on Cathodic Copper Plate Surface

- **Immature electrolytic processing leads to small particles discretely distributed on the surface of copper plates**

Examples of Particle Defects

Manual Detection and Removal

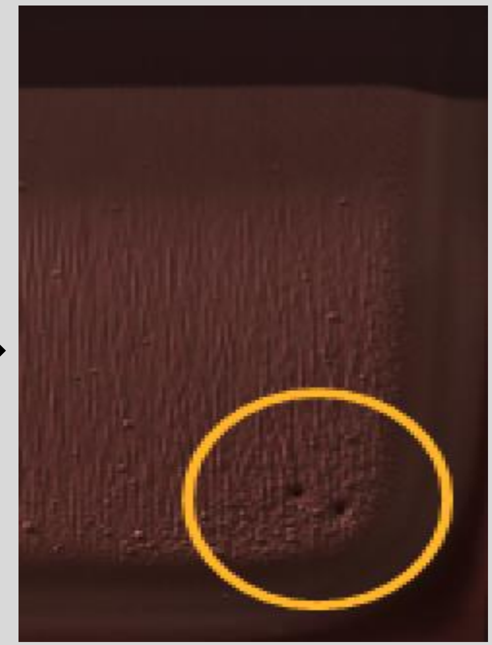

Copper Plates after Processing

- **Particles beyond the national standard (height exceeding the copper plate) are defects and need to be removed.**
- **Manual inspection and removal is time-consuming and laborious**

Introduction

■ Particle Defects on Cathodic Copper Plate Surface

- **Defects beyond the national standard (height exceeding the copper plate) will be detected and removed manually.**
- **To meet the requirements of intelligent manufacturing, an automatic defect detection method needs to be developed.**

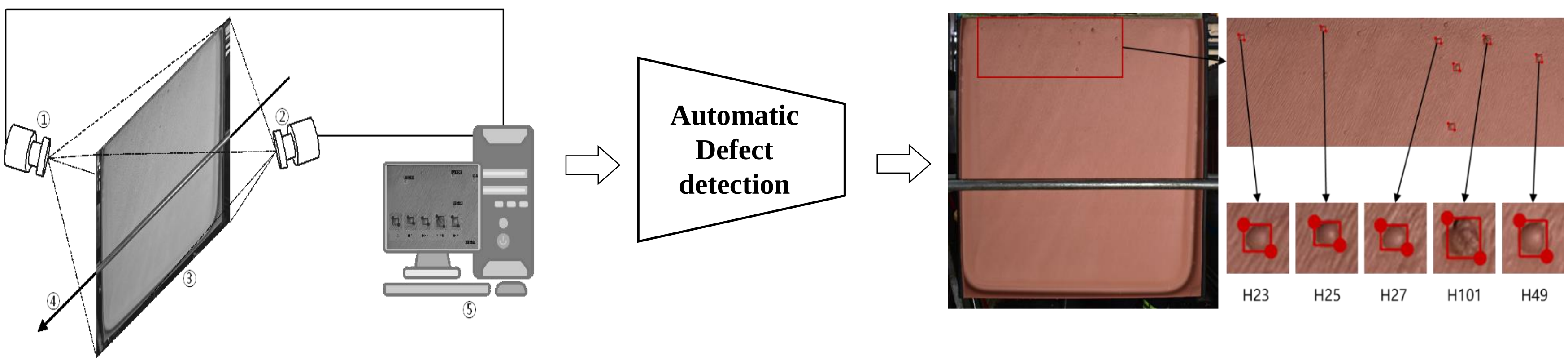

✓ **End-to-end manner**

✓ **Output: Location + Height**

Introduction

■ Deep learning Detection Model

- Anchor-based methods are most representative detection models and have shown high detection accuracy.

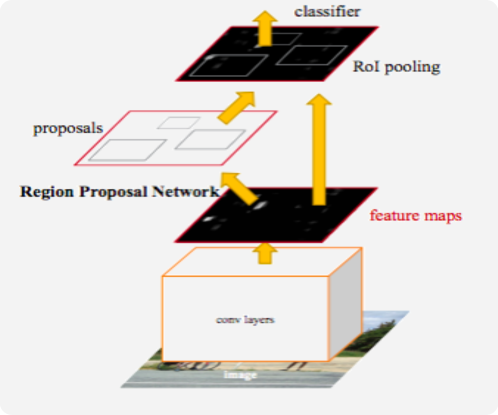

Faster RCNN

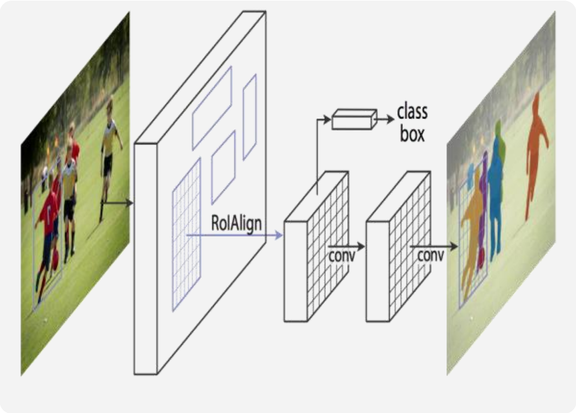

Mask RCNN

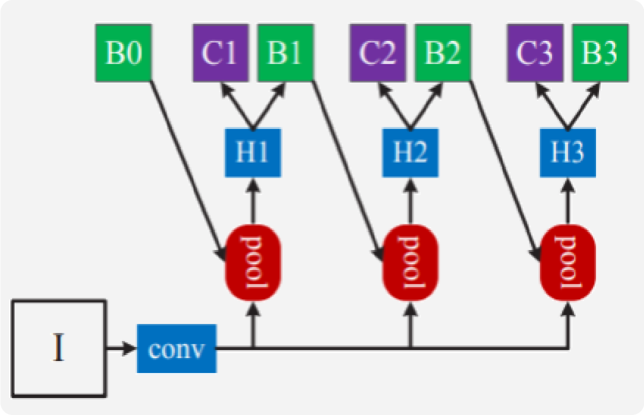

Cascade RCNN

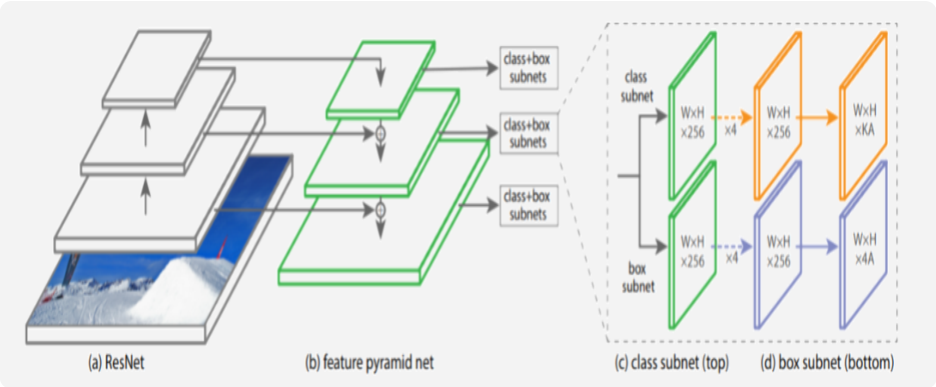

RetinaNet

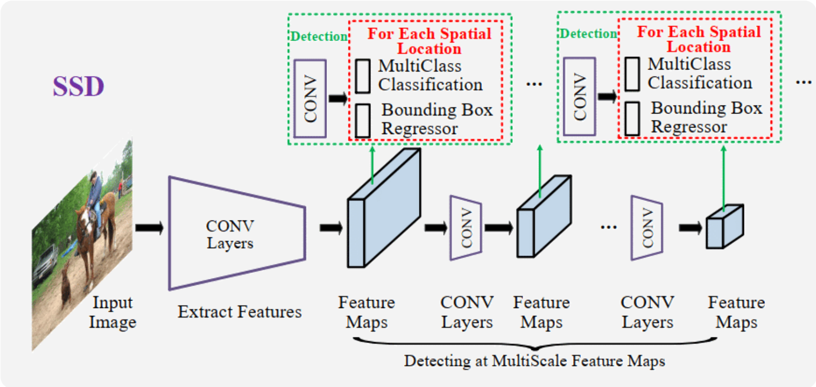

SSD

Introduction

Anchor-based Model for Defect Detection

- **Anchor-based models have been used in different industrial tasks, such as steel defect detection, PCB inspection.**

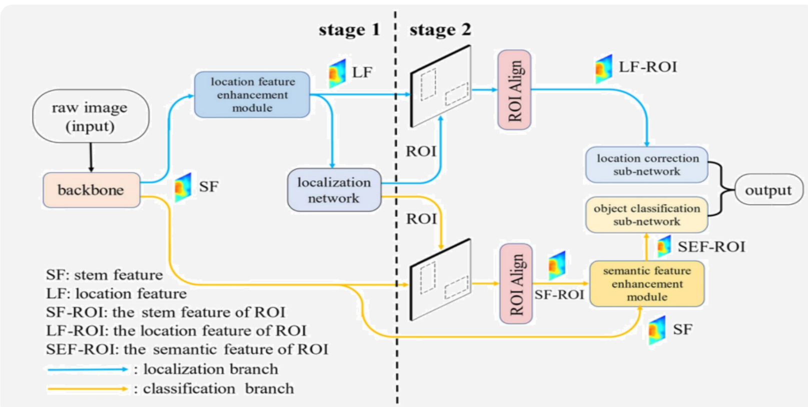

FPCB-DET

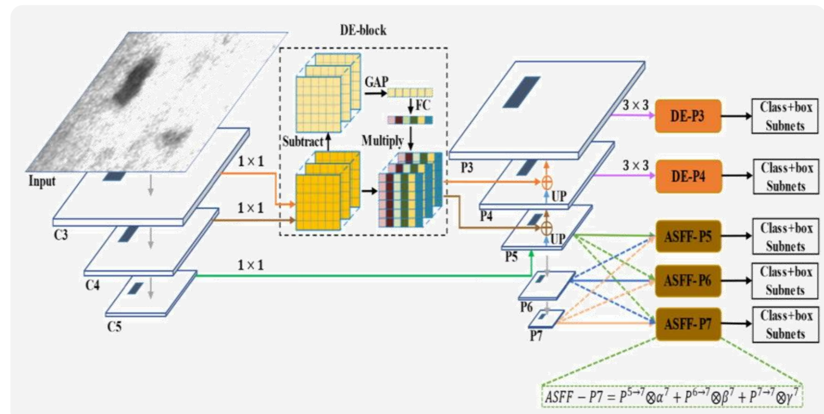

DEA-Retina Net

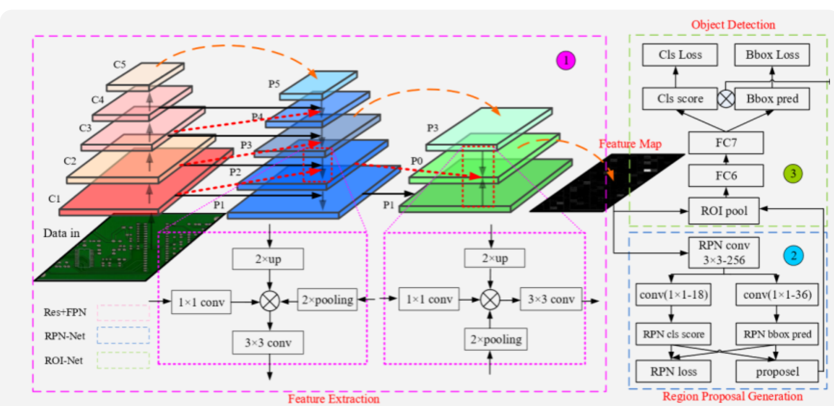

Extended FPN

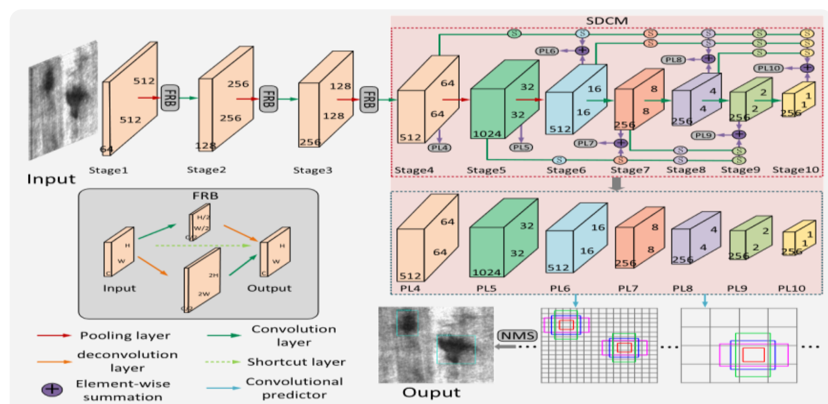

SDDNet

Introduction

■ Challenges for Copper Particle Defect Detection

General Problem

Large Scale vs Small Objects

PCB Inspection

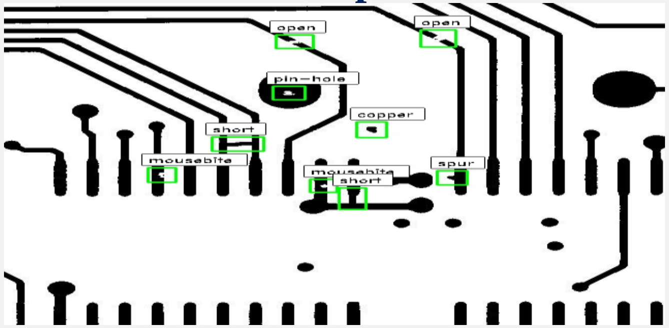

Copper Particle Detection

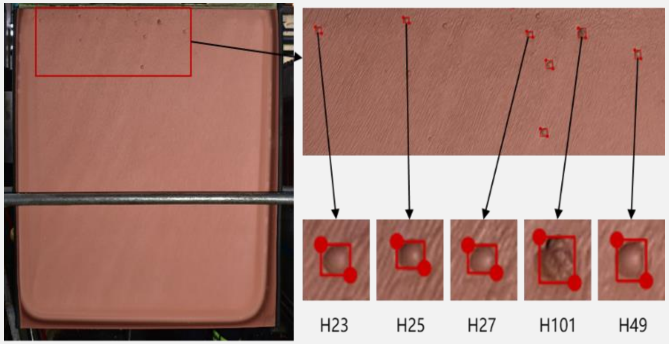

Specific Requirement

Multi-task design

- ✓ Category classification
- ✓ Objection localization

- ✓ One-category classification
- ✓ Objection localization
- ✓ Height Estimation

Proposed ADHE Method

■ Anchor-based Detection and Height Estimate Framework

- ADHE framework consists of three modules:
  - ◆ Image Block
  - ◆ Defect Region Extraction
  - ◆ Height-RCNN

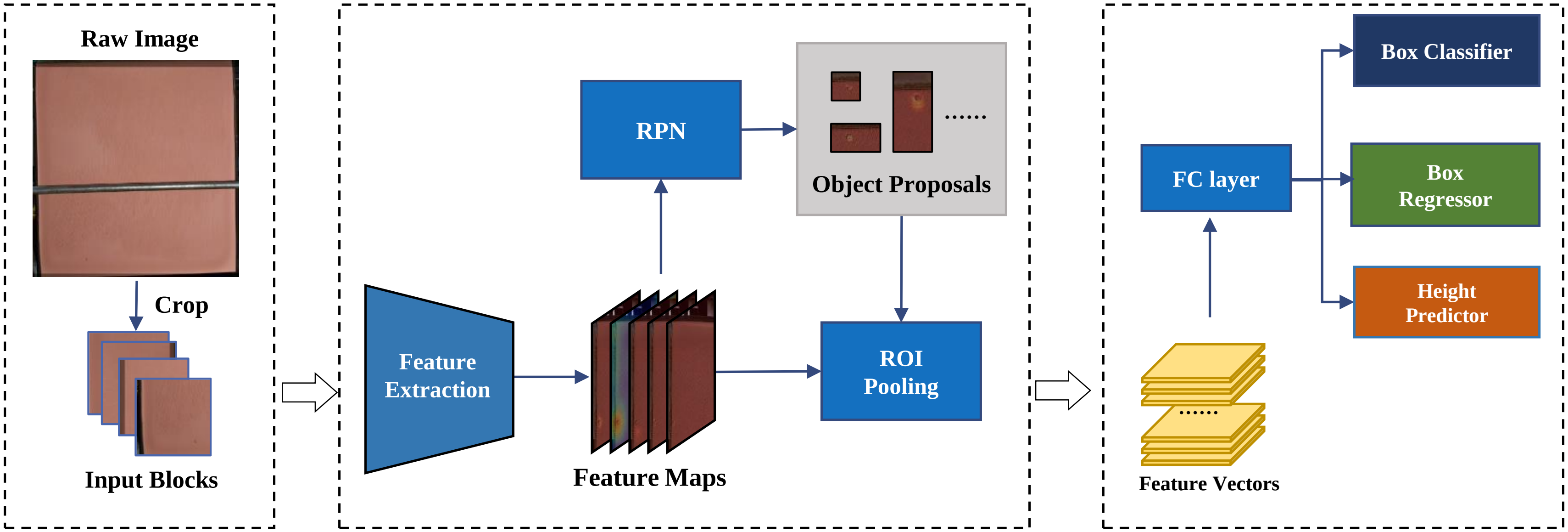

(a) Image Block (b) Defect Region Extraction (c) Height RCNN

Proposed ADHE Method

Image Block

- **Large-scale images cannot be directly fed into networks due to hardware limitations, so an image block operation is firstly adopted.**
- **Operation Parameters:**

  h: the height of a image block; w: the width of a image block

  s_h: the step between blocks in height direction

  s_w: the step between blocks in width direction

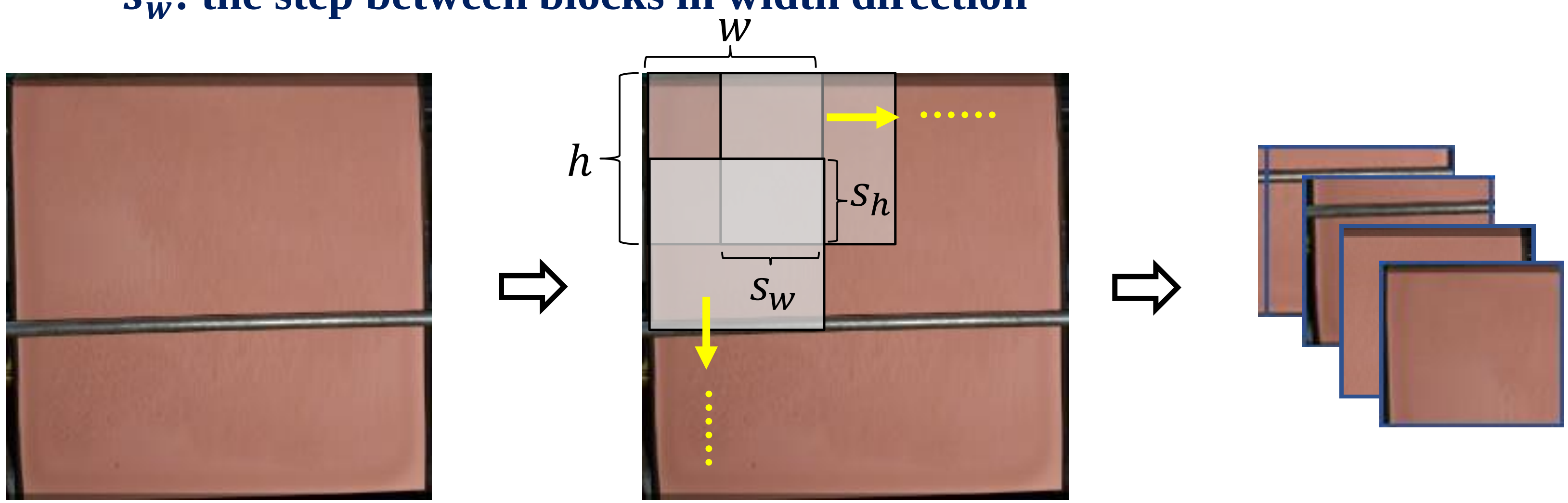

- **The receptive fields for small defects are adjusted and numbers of the training set are enlarged (oversampling)**

Proposed ADHE Method

■ Defect Region Extraction

- To accurately locate the defects and compute defect features in image blocks, an anchor-based method is deployed, including high-resolution feature extraction network, RPN network, and ROI Pooling.

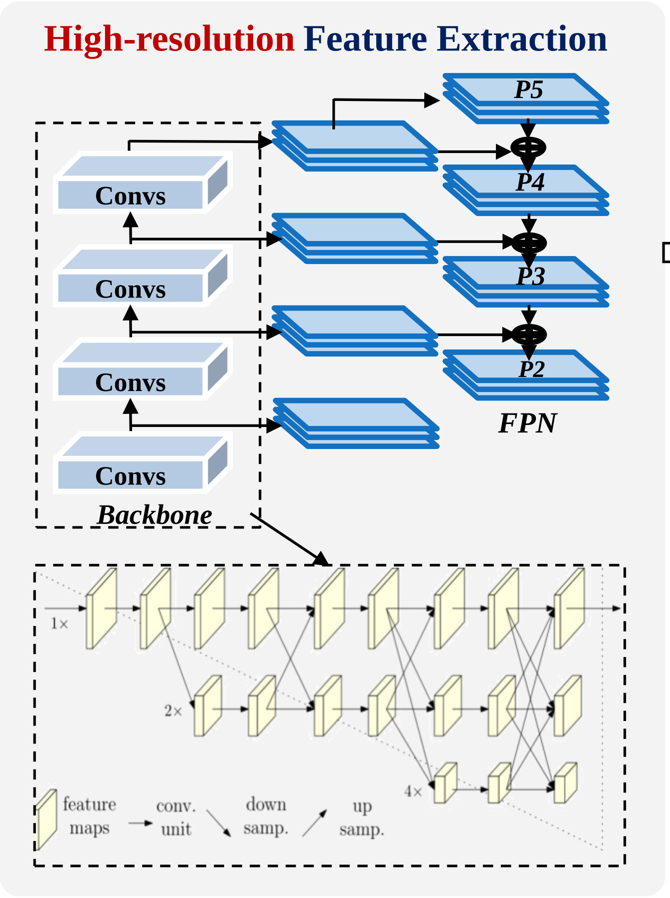

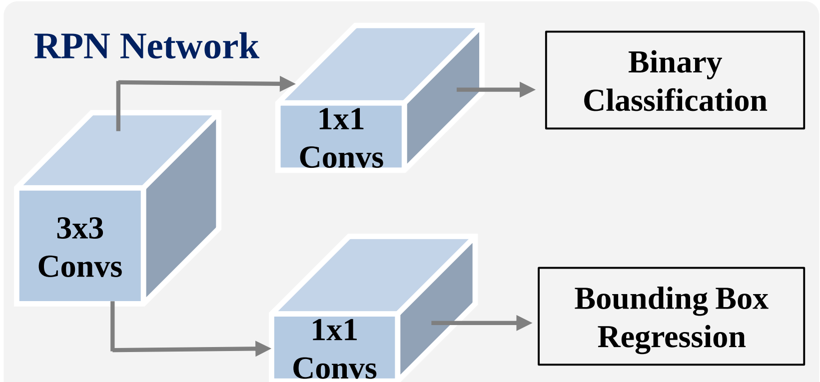

$$L_{RPN} = \frac{1}{N_{cls}}\sum_i L_{cls}(p_i, p_i^*) + \lambda_1 \frac{1}{N_{reg}}\sum_i p_i^* L_{reg}(t_i, t_i^*)$$

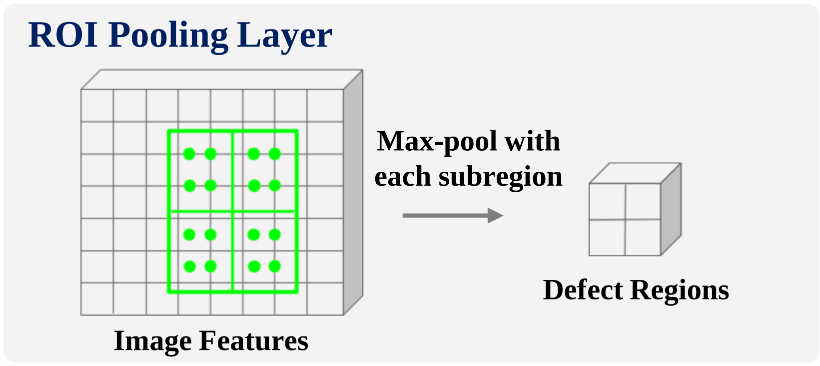

Proposed ADHE Method

■ Height RCNN (H-RCNN)

- Three separate branches are designed in H-RCNN to locate, classify defects and estimate their height in an end-to-end manner.

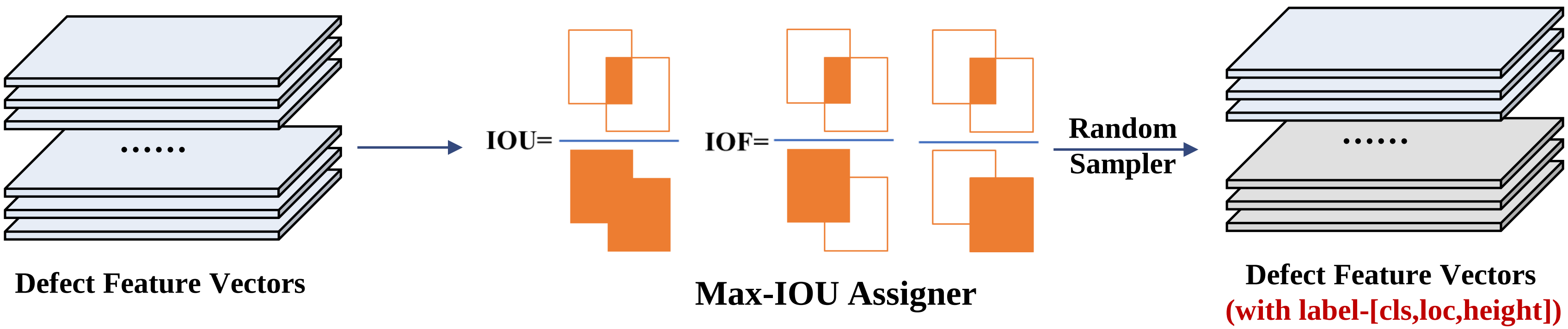

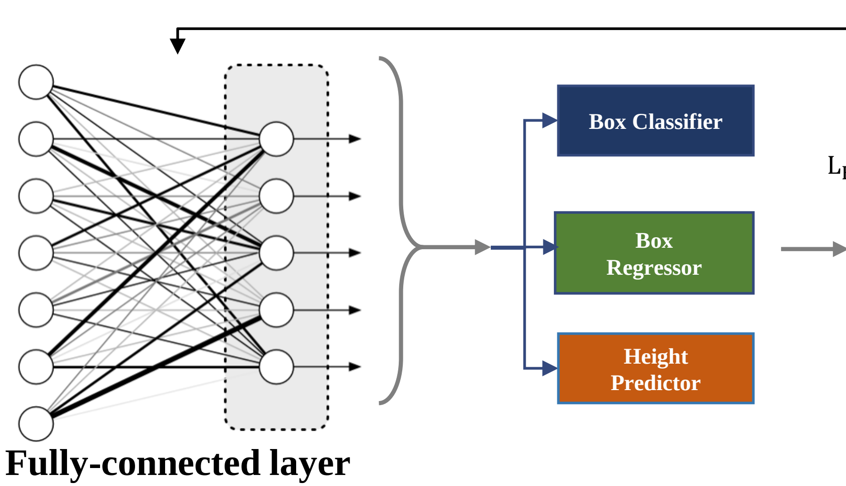

$$\mathrm{L}_{\mathrm{H-RCNN}} = \frac{1}{N_{bcls}}\sum_i L_{bcls}(u_i, u_i^*) + \lambda_2 \frac{1}{N_{breg}}\sum_i u_i^* L_{breg}(t_i, t_i^*) + \lambda_3 \mathrm{L}_{\mathrm{Height}}$$

$$\mathrm{L}_{\mathrm{Height}} = \frac{1}{N_{height}}\sum_i u_i^* L_{reg}(d_i, d_i^*)$$

Experiments

Dataset Description

- Cathodic Copper Plates Defect Dataset (CCPD) consists of 160 images collected from the real-world industrial copper manufacturing factory.
- Defects on each image are labeled with **category, location and height**.
- The resolution of each image is 2516×2428, and most defect objects are **extremely small** (less than 2000 pixels).

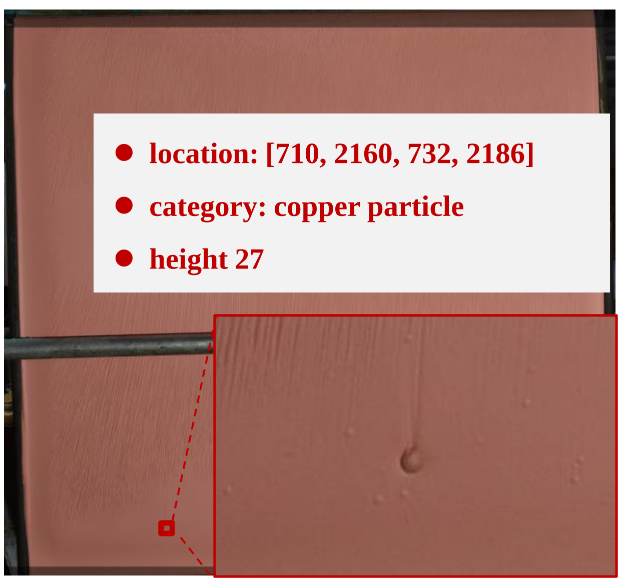

Annotation Example

Information of the Copper Particle dataset

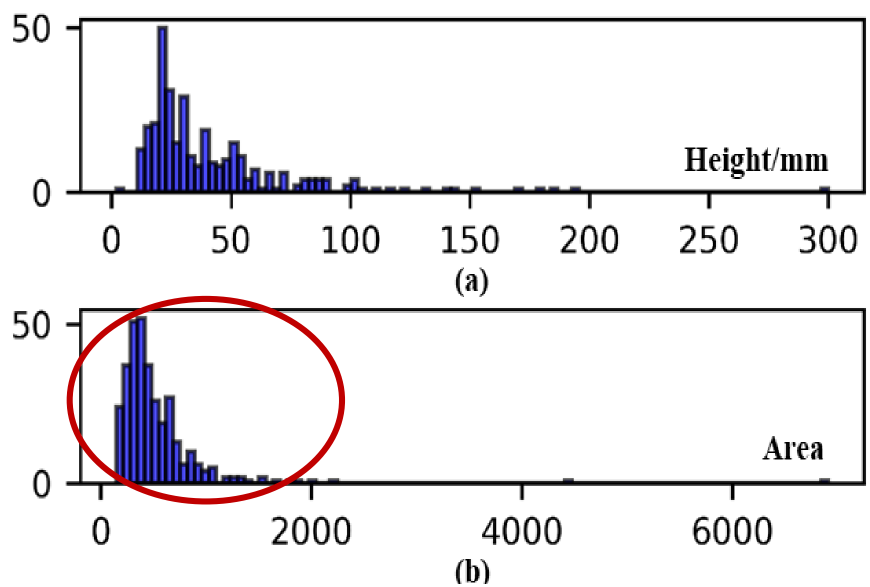

Experiments

Experimental Setup and Implementation Details

Implementation Details:

- **The default feature extraction network is HRNet-w40**
- **All the methods in these experiments run ten times with 20 epochs.**
- **The experiment is implemented by PyTorch and based on a single NVIDIA GeForce RTX 3090.**

The experiments include three parts:

- **The first part is comparison with conventional feature extraction.**
- **The second part is the influence of Image Block operations.**
- **The third part is the influence of hyperparameter in loss function**

Experiments

Evaluation Metrics

$$Recall = \frac{TP}{TP + FN}$$

$$Precision = \frac{TP}{TP + FP}$$

$$AP = \int_0^1 P(R)dR$$

$$RMSE = \sqrt{\sum_{i=1}^{n} \frac{(\hat{y}_i - y_i)^2}{n}}$$

TP and TN are short for true positive and true negative, and FP and FN denote the false positive and false negative. For Recall, Precision and Average Precision, the best value is 1 and the worst is 0. For RMSE, the smaller value is better

Experiments

■ Comparison with Conventional Feature Extraction

Method	Params	Detection			Height Estimation
		Precision↑	Recall↑	AP_{50}↑	RMSE↓
ResNet-50	26.63M	0.372	1.000	0.949	9.135
ResNet-101	45.62M	0.383	1.000	0.955	9.640
HRNet-w32	32.38M	0.379	1.000	0.951	10.016
HRNet-w40	48.63M	**0.393**	**1.000**	**0.956**	**8.572**

Detection: According to AP50 results, the detection performance gets better when models go bigger. And ADHE with HRNet-w40 achieves the highest AP value.

Height Estimation: Based on the well-learned features from the backbone, HRNet-w40 also achieves the best result on the height estimation task.

Experiments

Comparison with Conventional Feature Extraction

Feature Map Visualization with 4 different backbones

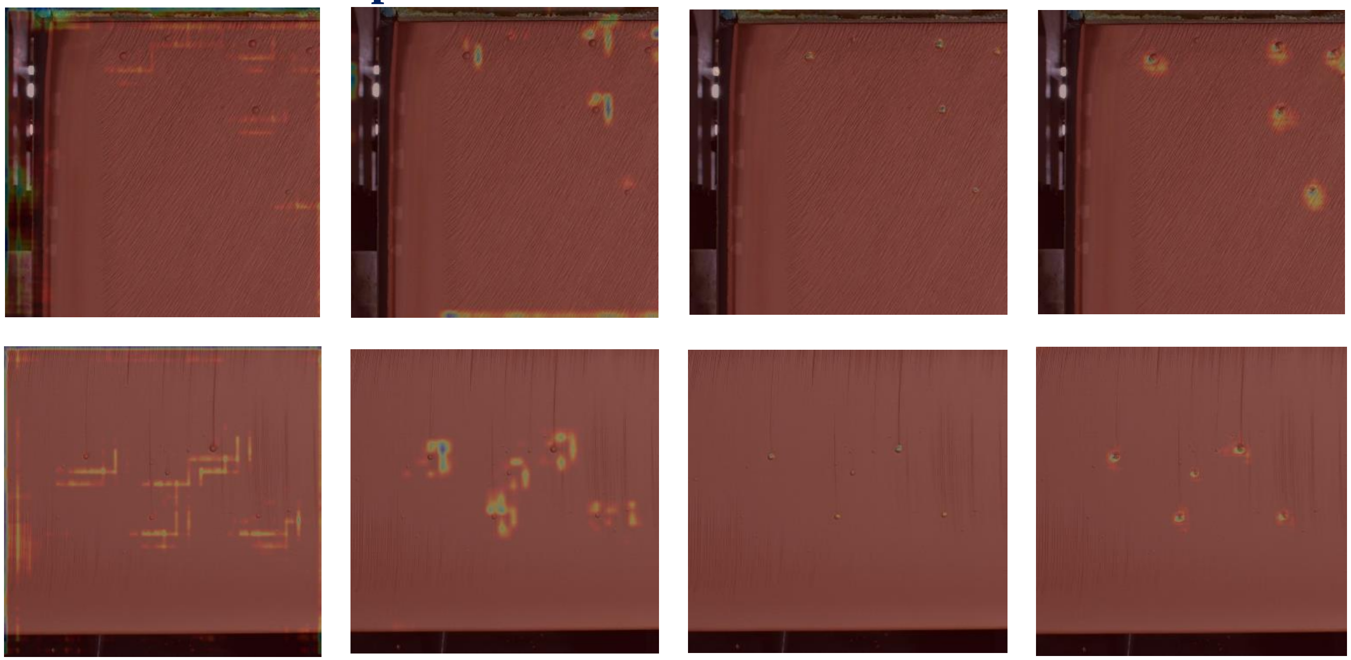

ResNet-50 ResNet-101 HRNet-w32 HRNet-w40

- **Between different model-class:** HRNet-based methods is better than ResNet-based methods, which locate more accurately and less active to useless backgrounds.
- **Between different model-size:** HRNet-w40 learns information from surrounding areas while HRNet-w32 only focuses on defect region, leading to performance gap

Experiments

■ The influence of Image Block operations

- **Setting:**

Sparse distribution→ $s_h = s_w = 0$ (no overlapping), $h = \frac{H}{n}, w = \frac{W}{n}$

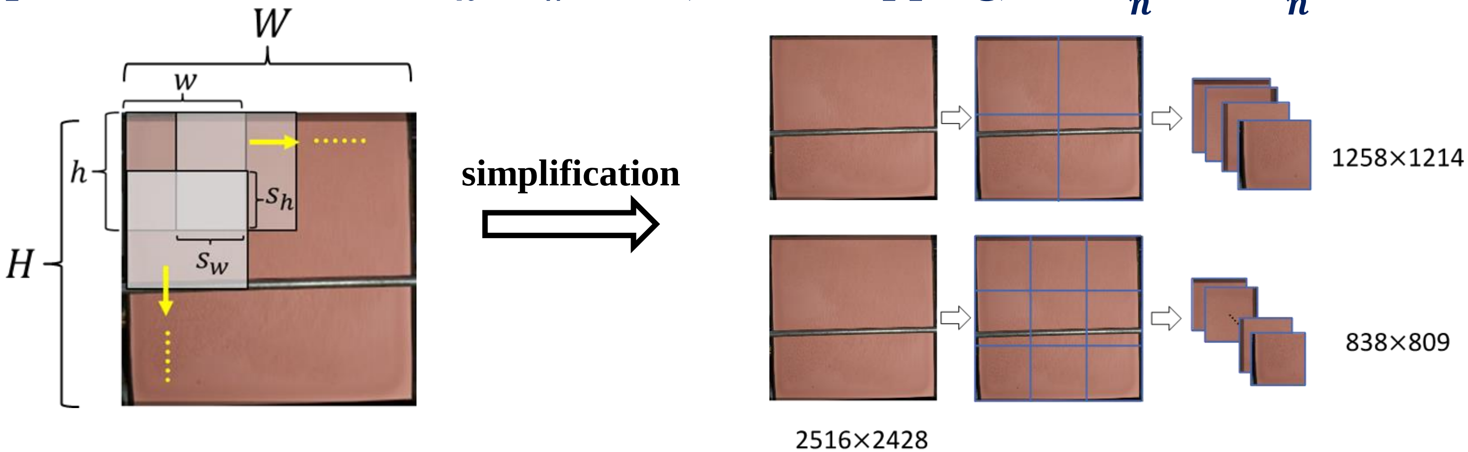

Block	Image Size	Image Number	Instance Number	Detection			Height Estimation
				Precision↑	Recall↑	AP_{50}↑	RMSE↓
1x1 (Raw)	**2516×2468**	**160**		**0.438**	0.767	0.715	13.127
2x2	**1258×1214**	**640**	**343**	0.392	0.971	0.927	12.314
3x3	**838×809**	**1440**		0.393	**1.000**	**0.956**	**8.572**

Between different block number: The detection and height estimation results get better when the block number adds

Experiments

■ Detection Visualization under Block 3×3

- The proposed method can accurately detect and locate the defect area, even the defect areas are small

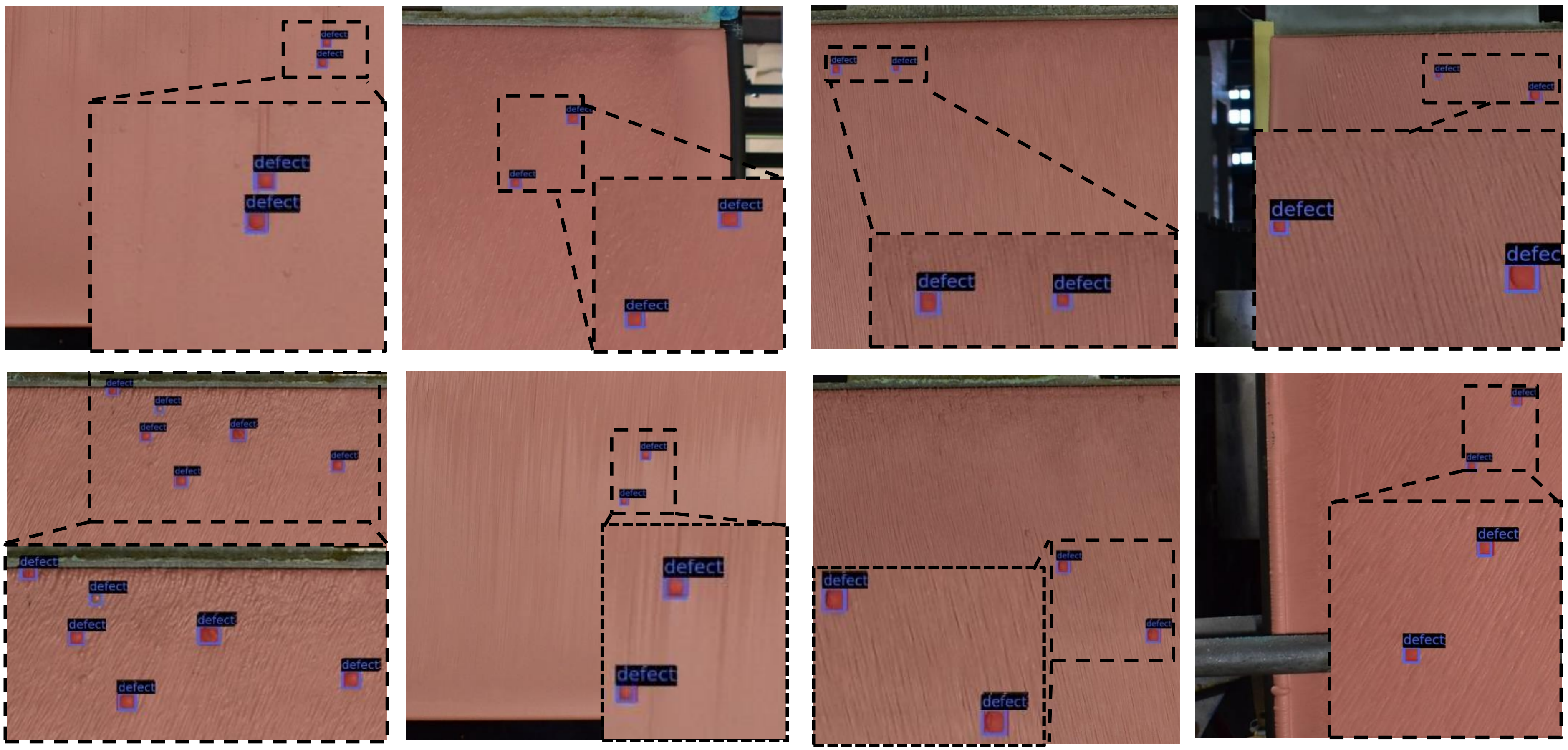

Ground truth boxes: purple area; Predicted boxes: blue boxes

Experiments

The Influence of Loss Hyperparameter λ_3

$$\mathrm{L} = \mathrm{L}_{\mathrm{RPN}} + \mathrm{L}_{\mathrm{RCNN}} + \boxed{\lambda_3}\mathrm{L}_{\mathrm{Height}} = \mathrm{L}_{\mathrm{RPN}} + \mathrm{L}_{\mathrm{RCNN}} + \boxed{\lambda_3}\frac{1}{N_{height}}\sum_i u_i^* L_{reg}(d_i, d_i^*)$$

λ_3	Detection			Height Estimation
	Precision↑	Recall↑	AP_{50}↑	RMSE↓
0.05	**0.395**	**1.000**	0.944	9.134
0.10	0.393	**1.000**	0.956	**8.572**
0.50	0.350	**1.000**	**0.962**	9.610
1.00	0.244	**1.000**	0.960	10.593
5.00	**0.395**	**1.000**	0.944	9.134

- **The best result on detection and height estimation cannot be achieved at the same time, a trade-off needs to be taken into consideration.**
- **0.1 is chosen as the default setting because it balances the training of both tasks and obtains a relatively better performance.**

Take-home Message

- **Conclusion:**
  - Image Block operation can crop large-scale raw images into several image blocks, which deals with the hardware limitation
  - A high-resolution feature extraction is helpful for small feature location and downstream task.
  - Height RCNN locate the defect out and estimates the height of the defect in an end-to-end way.

- **Limitations:**
  - The rate of image blocking requires human setting. It is significant to develop an adaptive image blocking method for defect detection and height estimation.
  - There are different background and light illumination of cathodic copper plates images. One of the research directions is to develop a domain adaptation ADHE method.

Acknowledgement

This work was supported by:

- **The National Key R&D Program of China under Grant 2018AAA0101700**

- **The National Natural Science Foundation of China under Grant 52188102**

Reference

[1] Y. Gao, X. Li, X. V. Wang, L. Wang, and L. Gao, "A Review on Recent Advances in Vision-based Defect Recognition towards Industrial Intelligence," J. Manuf. Syst., vol. 62, pp. 753–766, Jan. 2022.
[2] P. M. Bhatt et al., "Image-based surface defect detection using deep learning: A review," J. Comput. Inf. Sci. Eng., vol. 21, no. 4, 2021
[3] D. Carrera, F. Manganini, G. Boracchi, and E. Lanzarone, "Defect detection in SEM images of nanofibrous materials," IEEE Trans. Ind. Inform., vol. 13, no. 2, pp. 551–561, 2016.
[4] P. Bergmann, S. Löwe, M. Fauser, D. Sattlegger, and C. Steger, "Improving unsupervised defect segmentation by applying structural similarity to autoencoders," ArXiv Prepr. ArXiv180702011, 2018.
[5] I. Goodfellow et al., "Generative adversarial nets," Adv. Neural Inf. Process. Syst., vol. 27, 2014.
[6] J. Liu, C. Wang, H. Su, B. Du, and D. Tao, "Multistage GAN for fabric defect detection," IEEE Trans. Image Process., vol. 29, pp. 3388–3400, 2019.
[7] D. Mo, W. K. Wong, Z. Lai, and J. Zhou, "Weighted double-low-rank decomposition with application to fabric defect detection," IEEE Trans. Autom. Sci. Eng., vol. 18, no. 3, pp. 1170–1190, 2020.
[8] Y. He, K. Song, Q. Meng, and Y. Yan, "An End-to-End Steel Surface Defect Detection Approach via Fusing Multiple Hierarchical Features," IEEE Trans. Instrum. Meas., vol. 69, no. 4, pp. 1493–1504, Apr. 2020.
[9] H. Dong, K. Song, Y. He, J. Xu, Y. Yan, and Q. Meng, "PGA-Net: Pyramid feature fusion and global context attention network for automated surface defect detection," IEEE Trans. Ind. Inform., vol. 16, no. 12, pp. 7448–7458, 2019.
[10] S. Ren, K. He, R. Girshick, and J. Sun, "Faster R-CNN: Towards Real-Time Object Detection with Region Proposal Networks," IEEE Trans. Pattern Anal. Mach. Intell., vol. 39, no. 6, pp. 1137–1149, 2017.
[11] Y. Gao, L. Gao, and X. Li, "A Generative Adversarial Network Based Deep Learning Method for Low-Quality Defect Image Reconstruction and Recognition," IEEE Trans. Ind. Inform., vol. 17, no. 5, pp. 3231–3240, 2021.
[12] Y. Gao, L. Gao, X. Li, and X. V. Wang, "A multilevel information fusion-based deep learning method for vision-based defect recognition," IEEE Trans. Instrum. Meas., vol. 69, no. 7, pp. 3980–3991, 2019.
[13] K. He, G. Gkioxari, P. Dollar, and R. Girshick, "Mask R-CNN," 2017 IEEE International Conference on Computer Vision (ICCV). IEEE, 2017.
[14] L. Xiao, B. Wu, and Y. Hu, "Surface defect detection using image pyramid," IEEE Sens. J., vol. 20, no. 13, pp. 7181–7188, 2020.
[15] F. Li and Q. Xi, "DefectNet: toward fast and effective defect detection," IEEE Trans. Instrum. Meas., vol. 70, pp. 1–9, 2021.
[16] J. Luo, Z. Yang, S. Li, and Y. Wu, "FPCB surface defect detection: A decoupled two-stage object detection framework," IEEE Trans. Instrum. Meas., vol. 70, pp. 1–11, 2021.
[17] C. Li, Z. Qu, S. Wang, K. Bao, and S. Wang, "A Method of Defect Detection for Focal Hard Samples PCB Based on Extended FPN Model," IEEE Trans. Compon. Packag. Manuf. Technol., 2021.
[18] L. Liu et al., "Deep learning for generic object detection: A survey," Int. J. Comput. Vis., vol. 128, no. 2, pp. 261–318, 2020.
[19] R. Girshick, "Fast r-cnn," in Proceedings of the IEEE international conference on computer vision, 2015, pp. 1440–1448.
[20] W. Liu et al., "Ssd: Single shot multibox detector," in European conference on computer vision, 2016, pp. 21–37.
[21] T.-Y. Lin, P. Goyal, R. Girshick, K. He, and P. Dollár, "Focal loss for dense object detection," in Proceedings of the IEEE international conference on computer vision, 2017, pp. 2980–2988.

Thanks for Listening!